References and Notes

1. B. Digby, *The Mammoth and Mammoth-hunting in Northeast Siberia* (Appleton, New York, 1926).
2. I. P. Tolmachoff, *Trans. Am. Phil. Soc.* **23** (1929); this paper is the main source of information published prior to 1929.
3. I. T. Sanderson, *Saturday Evening Post* **39** (16 Jan. 1960).
4. I. Velikovsky, *Earth in Upheaval* (Doubleday, New York, 1955), chap. 1; C. H. Hapgood, *Saturday Evening Post* **22** (10 Jan. 1959).
5. Most of the first-hand information on discovery and geology of the mammoths is still available only in Russian.
6. H. F. Osborn, *Proboscidea* (American Museum of Natural History, New York, 1942), pp. 1122–69.
7. A. S. Romer, *Vertebrate Paleontology* (Univ. of Chicago Press, Chicago, ed. 2, 1945), p. 415.
8. C. W. Hibbard, in R. F. Flint, *Glacial and Pleistocene Geology* (Wiley, New York, 1957), p. 464.
9. H. C. Ezra and S. F. Cook, *Science* **129**, 465 (1959).
10. J. K. Charlesworth, *The Quaternary Era* (Arnold, London, 1957).
11. R. Carrington, *Elephants* (Basic Books, New York, 1959).
12. R. F. Flint, *Glacial and Pleistocene Geology* (Wiley, New York, 1957).
13. W. Soergel [*Palaeontol. Z.* **22** (1941)] treats the climatic significance of the *meridionalis-trogontherii-primigenius* line; K. D. Adam, *Geol. Bavarica No. 19* (1953), pp. 357–363.
14. A. Heintz, *Blyttia* **16**, 122 (1958), a paper based on pollen analyses by Kuprijanova; F. Camus, *Compt. rend.* **160**, 842 (1915). H. Gams [in F. Verdoorn, *Manual of Bryology* (Nijhoff, The Hague, 1915), p. 313] comes to the same conclusion on the basis of mosses.
15. L. S. Quackenbush, *Bull. Am. Museum Nat. Hist.* **26**, 107 (1909).
16. Horse, steppe bison, giant deer, woolly rhinoceros, arctic musk ox, and reindeer are open-terrain, cold-latitude animals which often occur with *M. primigenius*; warmer-latitude woodland types such as woodland musk ox, stag, and elk are less common associates (data from numerous sources).
17. W. Soergel, *Palaeontol. Z.* **22**, 33, 40 (1941).
18. E. M. Kindle, *Am. J. Sci.* **208**, 183 (1924) (for Banks Island); J. R. Mackay, *Can. Dept. Mines and Tech. Surveys, Mines Branch Mem. No. 5* (1958), p. 25 (for MacKenzie River delta area).
19. H. E. Anthony, *Natural Hist.* **58**, 299 (1949).
20. A. J. Popov, in *The Ice Age in the European Section of USSR and in Siberia*, K. K. Markov and A. J. Popov, Eds. (State Lomonosov Univ. of Moscow, 1959), p. 259 (in Russian).
21. Y. D. Zaklinskaya, in *ibid.*, p. 276; A. P. Zhuze, in *ibid.*, p. 301; E. N. Pavlovskij, *Proc. Intern Congr. Zool., 14th Congr.* (1956), p. 61.
22. V. N. Saks and S. A. Strelkov, "Quaternary Deposits of the Soviet Arctic," *Trans. Arctic Geol. Research Inst. Moscow* **91**, 221 (1959) (in Russian).
23. H. R. Crane, *Science* **124**, 670 (1956).
24. E. A. Olson (Lamont Geological Observatory), personal communication; this mammoth was first reported by H. E. Anthony [*Natural Hist.* **58**, 299 (1949)].
25. A. P. Vaskovsky, in *Ice Age in the European Section of USSR and in Siberia*, K. K. Markov and A. J. Popov, Eds. (State Lomonosov Univ. of Moscow, 1959), p. 512, Fig. 1.
26. M. Stuiver, E. S. Deevey, L. S. Gralenski, *Am. J. Sci. Radiocarbon Suppl.* **2**, 53 (1960).
27. E. S. Deevey and R. F. Flint, *Science* **125**, 182 (1957).
28. V. D. Dibner, in V. N. Saks and S. A. Strelkov [*Trans. Arctic Geol. Research Inst. Moscow* **91**, 98, Fig. 8 (1959)] also assigns the Mamontova fauna to the Karginsky interstadial, and therefore prior to the end of the last glaciation.
29. L. A. Kuprijanova, in A. Heintz, *Blyttia* **16**, 139 (1958); see Heintz's counterarguments in the same paper.
30. J. B. Griffin, *Science* **131**, 802 (1960).
31. Benkendorf and Hertz, cited in B. Digby, *The Mammoth and Mammoth-hunting in Northeast Siberia* (Appleton, New York, 1926), pp. 102, 118–19.
32. E. W. Pfizenmayer, *Mammutleichen und Urwaldmenschen in Nordost-Siberien* (Brockhaus, Leipzig, 1926), p. 167.
33. Three of the four known frozen rhinoceroses were found south of the Arctic Circle, and the animals did not cross the Bering Strait. They were probably animals of warmer climate than the mammoths.

34. This article is Lamont Geological Observatory contribution No. 480. It was supported by a grant from the U.S. Steel Foundation. The subject was suggested and valuable advice was offered by M. Ewing and W. L. Donn of Lamont Geological Observatory. C. W. Hibbard and W. S. Benninghoff of the University of Michigan gave a great deal of help with biological details. H. E. Anthony and R. G. Van Gelder of the American Museum of Natural History were very helpful in supplying parts of the frozen baby mammoth for radiocarbon dating.

Debris from Tests of Nuclear Weapons

Activities roughly proportional to volume are found in particles examined by autoradiography and microscopy.

Jan Sisefsky

Since the summer of 1955, airborne debris from nuclear-weapon tests has been collected and examined at the Research Institute of National Defence, Stockholm. The debris has been collected on glass-fiber paper (30 by 60 cm) with a sampling device carried by aircraft (*1*) at altitudes up to about 13 kilometers. Usually two samples have been taken at the same time, one above and one below the tropopause. Debris has also been collected on glass-fiber paper at ground level.

Routinely, one-fourth of the filter paper is used for spectrometric determination of the contents of a number of gamma-ray-emitting nuclides, from which an age determination can be made (*2*). The remainder is autoradiographed on photographic film of the type most sensitive to beta rays—that is, no-screen x-ray film (*3*, p. 220) (Ilford "Ilfex"). The exposure time is usually 7 days, and the films are developed according to the recommended procedure (ID 42; 4 minutes, 20°C). The autoradiographs show black, dense, circular spots with diffuse edges, varying in diameter from a few millimeters down to about 10 microns (see Fig. 1); spots of 10-micron diameter are the smallest that can be distinguished. The largest spots appear only when there is fresh radioactivity; usually only a few of them appear per square decimeter of filter area. The smaller spots are more frequent, the smallest ones being sometimes so numerous that they merge to a black haze, reproducing the structure of the filter. Although, as a rule, samples taken above the tropopause are of higher activity than the corresponding ones taken below it, the ratio of big spots to small ones is usually larger for samples taken below the tropopause.

From the autoradiographs it is possible to determine the activity of the individual particles and to locate their position on the filter (see *4*).

The author is affiliated with the Research Institute of National Defence, Stockholm.

Radioactive Particle Measurement

The simplest method of measuring the size of an autoradiograph spot is to determine its "diameter" under the microscope with a low-power objective (for example, × 4; ocular, × 12.5) and an ocular scale. The totally black center of a spot is surrounded by an area where the unexposed parts lie like islands in the blackening area. Further out from the center the black grains lie isolated, surrounded by unexposed film (Fig. 1). The edge of a spot can be defined as the zone where these two types of blacken-

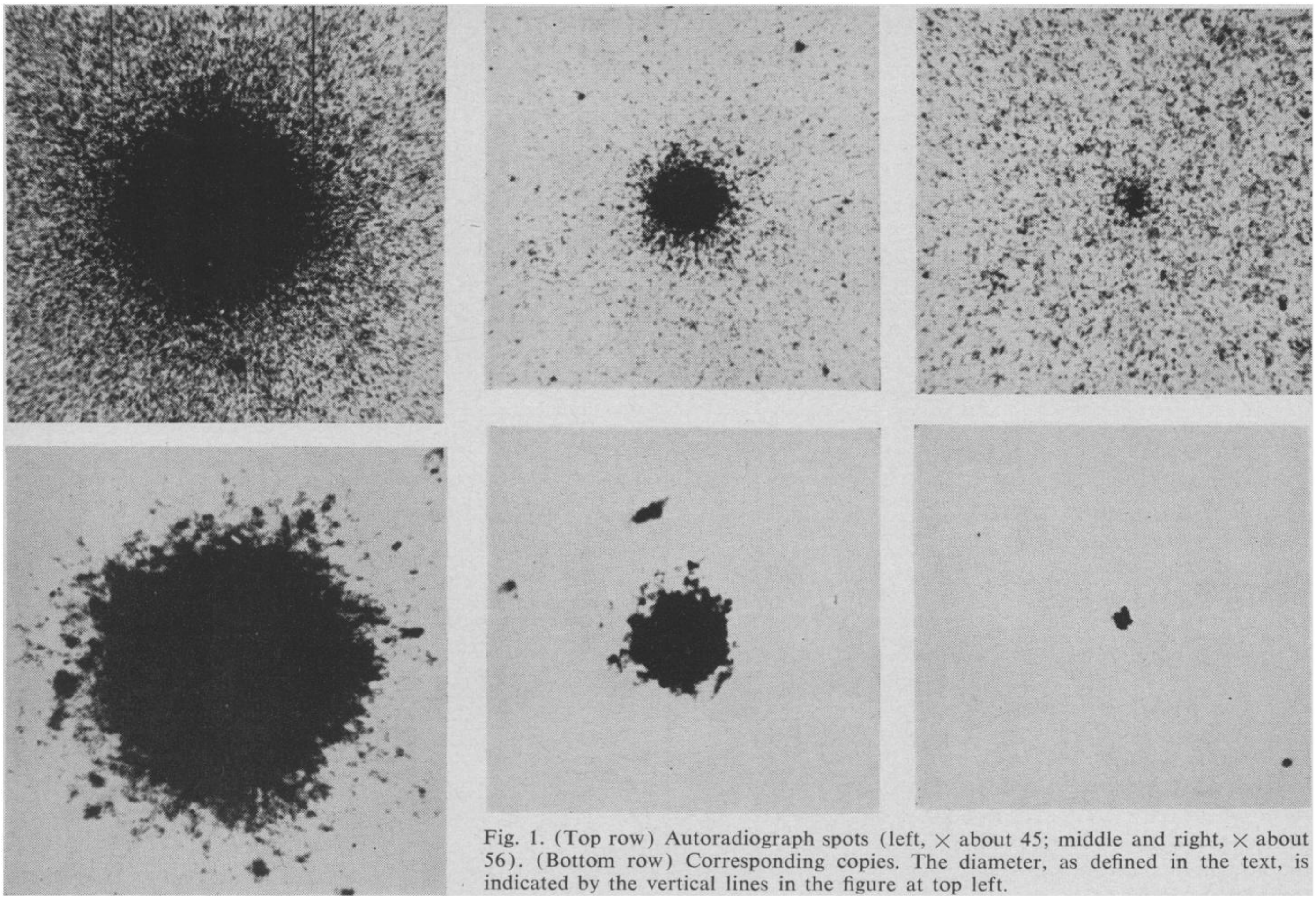

Fig. 1. (Top row) Autoradiograph spots (left, × about 45; middle and right, × about 56). (Bottom row) Corresponding copies. The diameter, as defined in the text, is indicated by the vertical lines in the figure at top left.

ing change. In this way, an approximate diameter of even very small spots can be defined. The reproducibility is about 5 to 10 percent for a spot exceeding 200 microns if the measurements are made by the same observer. Sizes of the smallest detectable spots (10 to 20 μ) can be estimated within a factor of 2. The spots may also be made more sharp-edged if they are copied onto high-contrast photographic film (Fig. 1). This process must be carefully standardized; otherwise each copy must be calibrated with standard spots.

Suppose, now, that there is a radioactive point source on a photographic emulsion film of negligible thickness. The radiation will diminish with increasing distance from the point source by at least the square of the distance, as the radiation is absorbed in the film. At a certain distance from the source, the radiation will be just strong enough to cause a blackening, characterizing the limiting zone defined above.

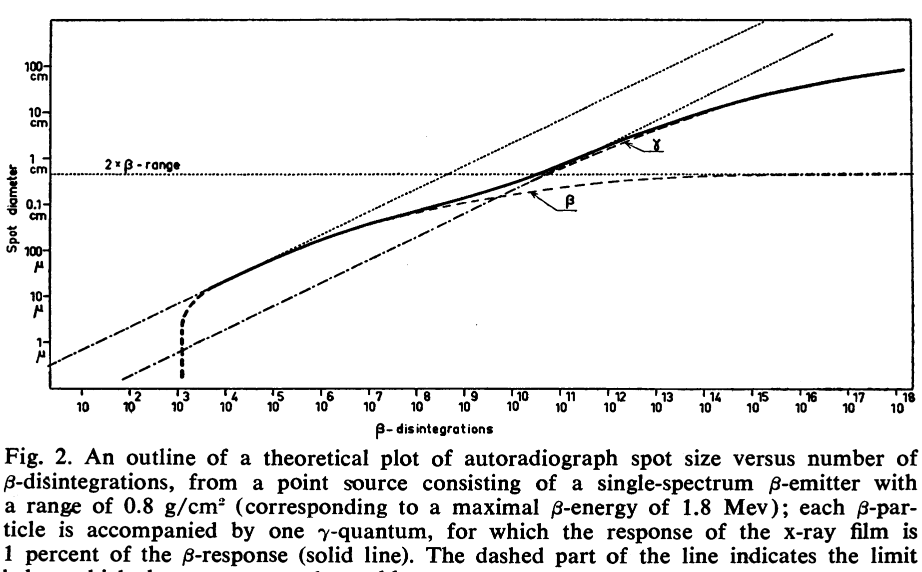

Fig. 2. An outline of a theoretical plot of autoradiograph spot size versus number of β-disintegrations, from a point source consisting of a single-spectrum β-emitter with a range of 0.8 g/cm^2 (corresponding to a maximal β-energy of 1.8 Mev); each β-particle is accompanied by one γ-quantum, for which the response of the x-ray film is 1 percent of the β-response (solid line). The dashed part of the line indicates the limit below which the spots are undetectable.

For a small spot we need consider only the β-radiation [the α-radiation of nuclear-weapon debris is negligibly weak and the γ-radiation has a blackening power only a few percent of that of the β-radiation (3, p. 18)]. Further, if we consider a spot of such small radius that the β-absorption in the emulsion and the change in the β-energy are negligible, we have in the edge zone of the spot:

$$S = K \cdot \frac{It}{d^2}$$

Therefore

$$d = K\,(It)^{\frac{1}{2}}$$

where S is the edge-zone blackening, I is the β-intensity, t is the exposure time, and d is the diameter of the spot, and K is a constant. If we plot the spot diameter versus the number of emitted β-particles on a log-log scale, the plot will start as a straight line with the slope

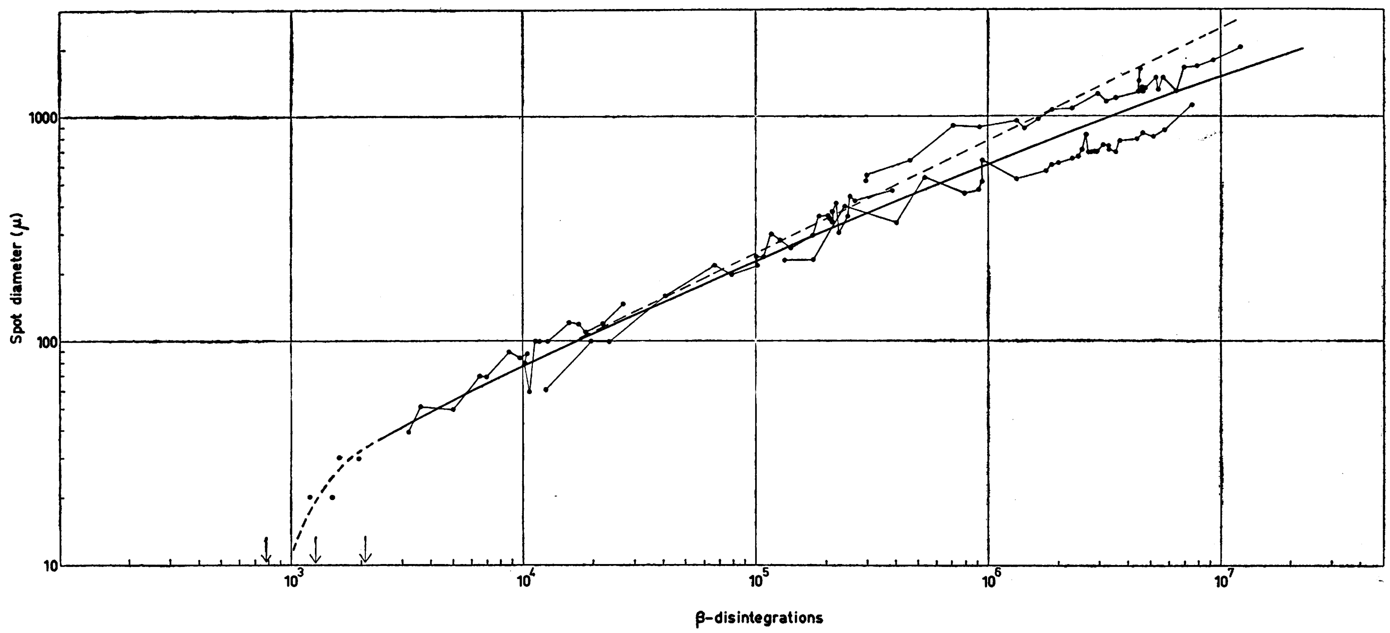

Fig. 3. Some typical plots of spot size versus activity for a set of nuclear-debris particles, showing the displacement effect (connected points) and the average plot (used for calibration purposes). The heavy line is compared with a line with the slope ½ (thin dotted line).

½. For larger spots we must consider the β-absorption in the emulsion as well as the change in the β-energy spectrum of the radiation. This will, of course, cause the curve to deviate from the straight line and to approach asymptotically the horizontal line corresponding to twice the maximum β-range for the radiation in question.

However, we must now also consider the γ-radiation, which will be predominant at long distances from the source. Since a monoenergetic γ-flux from a point source decreases approximately according to the law

$$I = \frac{I_0 \cdot e^{-\mu r}}{r^2}$$

where μ is the absorption coefficient and r is the distance from the source, the γ-radiation will cause the curve to rise again toward infinity but with a steadily decreasing slope (Fig. 2).

An attempt is being made to demonstrate these relationships by using different β- and γ-emitting nuclides as point sources. For the studies under discussion, nuclear-debris particles emitting radiation strong enough to be measured in β-counters (stronger than 10 to 20 disintegrations per minute) were used to determine the connection between activity and spot size. However, it turned out that the spot-size–activity plots were horizontally displaced from one x-ray film to another, even when the films were from the same box and the temperatures and processing times were carefully controlled (Fig. 3). This

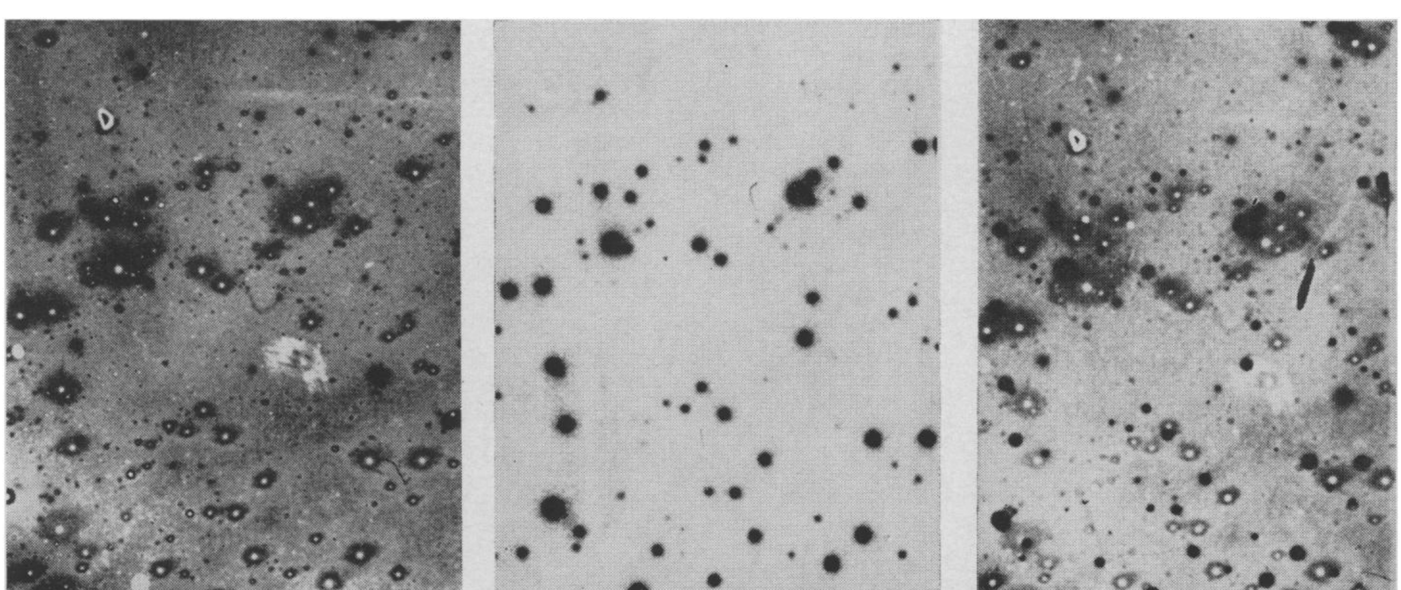

Fig. 4. (Left) A portion of a particle-plate coated with emulsion. The particles are found in the centers of the clear spots surrounded by dark rings. (Middle) The corresponding x-ray film autoradiograph. (Right) Copies of the left and center photographs superimposed, with a slight displacement. (About × 3.4)

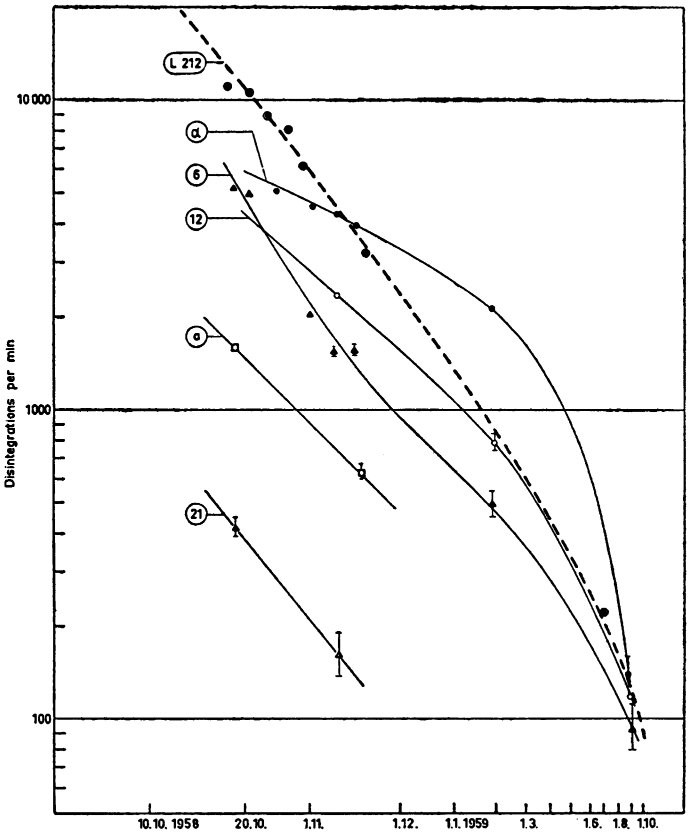

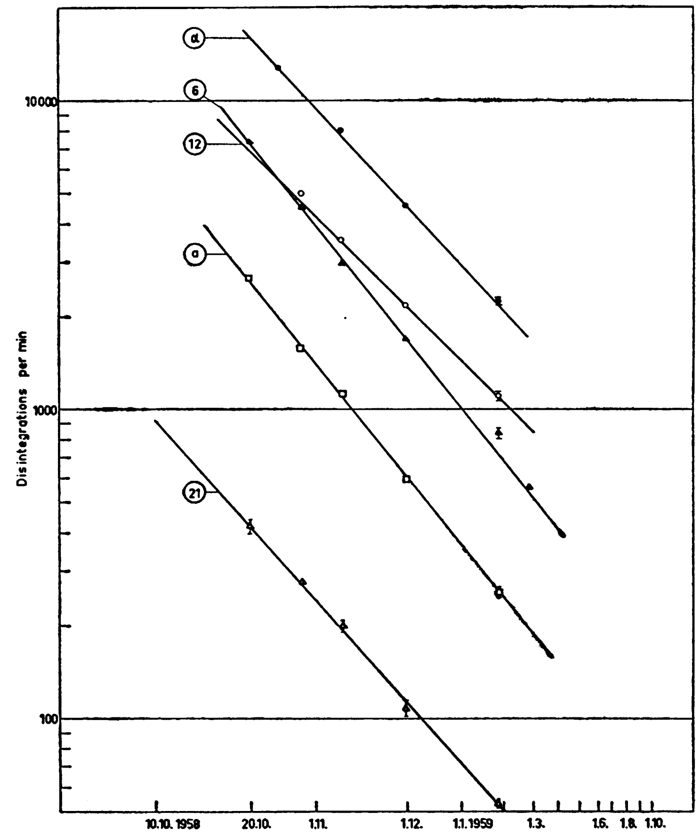

Fig. 5 (left). Some representative γ-decay curves, and a more anomalous curve (*6*) for single particles compared with the γ-decay curve for all radioactivity in sample L-212 (dotted line) sampled from 180 g of air. (Particles from sample L-211 are marked with letters; those from L-212 with numbers.) Gamma disintegrations per minute are calculated from γ-counts per minute simply by dividing by an average efficiency (7 percent), as the efficiency for the average energy of fission products probably does not vary more than 20 percent for the ages in question (*2*). Fig. 6 (right). Curves for β-decay for the same fallout particles as in Fig. 5.

made it necessary to normalize the plot for each film by means of β-measurements of a few particles.

By this method the β-activity of particles from nuclear debris can be estimated with an accuracy of about 10 to 20 percent down to approximately 3000 disintegrations during the exposure time; 1000 disintegrations are needed to produce a detectable spot (and the activity is then estimated by a factor of 2 to 3). If the exposure time is 1 week, the corresponding disintegrations per minute are 0.3 and 0.1, respectively.

It may be of interest to compare this method with ordinary β-measurements. A low-background anticoincidence β-counter, such as the one now in use in this laboratory (*5*), with 15 percent efficiency and background activity of 0.3 count per minute, requires 2 days to measure the activity of a particle with activity of 0.3 disintegration per minute with 20 percent accuracy. Since we were dealing with hundreds of particles with activity in the range of 0.1 to 10 disintegrations per minute, this procedure could not be used.

Microscopic Examination of the Particles

The method of microscopic examination used, described in detail elsewhere (*4*), is, briefly, as follows. The particles are transferred to celluloid films on glass plates. They are then covered with nuclear emulsion in gel form, which is "reversal-developed" by a special method that gives clear, circular autoradiograph spots against a brown transparent background. In the centers of these spots the active particles can be seen in the microscope. An ordinary x-ray autoradiograph is made simultaneously for use in activity determinations. (The clear circles on the plate are not suitable for this purpose because of their irregular size, due to the varying thickness of the hand-cast emulsion layer.)

If a great number of particles are to be examined on a plate, it may be profitable to transfer the x-ray film autoradiograph to the plate in the following way. The autoradiograph is copied onto a soft film (which gives a true negative without diminishing the sizes of the spots). This film is, in turn, contact-copied onto another film which should be of high contrast and thin (for example, Gevaert Dipos Contact). The copy, which shows the spots of the autoradiograph with greater contrast (at least for the smaller particles) is placed in close contact with the emulsion layer on the plate by means of immersion oil, so that the spots on the autoradiograph and the corresponding clear areas in the plate are adjacent to each other. The thin, clear film does not impede the examination of the active particles under

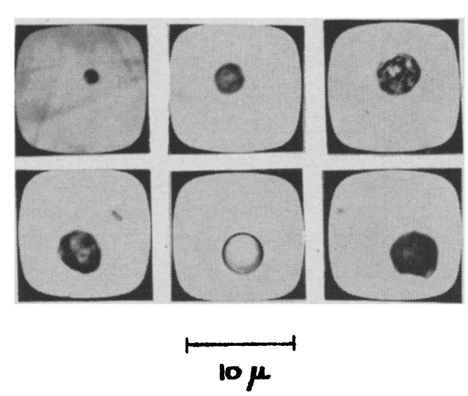

Fig. 7. Fallout particles from the Soviet bomb test of 30 September 1958.

the microscope, even if an immersion-oil objective is used (Fig. 4).

The particles are now visible under a microscope and can be identified by their positions in the clear areas (a low-power objective is used for larger areas). They are examined with the highest-power objective (oil objective, × 100; ocular, × 12.5), their diameters are measured by a calibrated ocular scale, and their color, form, and transparency are observed.

Soviet Bomb-Test Series of September-October 1958

The Soviet bomb-test series of September and October 1958 took place in Novaja Zemlja, beginning on 30 September with two explosions and continuing with several explosions during October. Seismic data (*6*) indicated that the most powerful explosions occurred on 18 and 22 October.

The radioactive debris was first observed by the Research Institute of National Defence in a ground air sample taken on 8 October 1958 in Stockholm. Nine days later, on 17 October, the debris was observed for the first time in a high-altitude sample. At a height of 12 kilometers over central Sweden a very strongly radioactive air sample (called L-212) was gathered (~ 30,000 pc/kg of air). (The count for the sample taken immediately prior to this, at the same height, was approximately

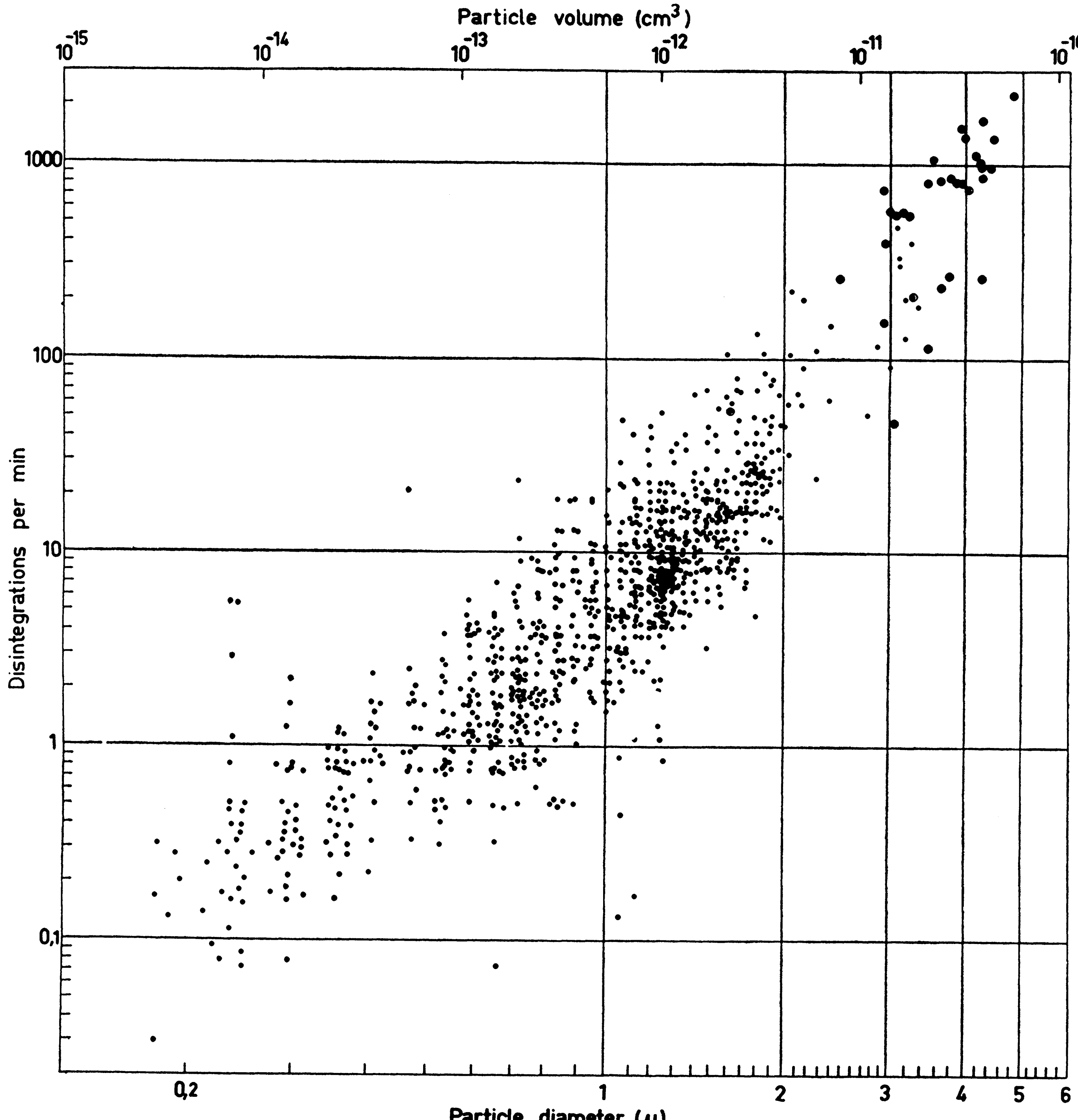

Fig. 8. Activity versus size for 950 particles from sample L-212 on 29 January 1958 at the age of 120 days. The particles measured in the β-counter are marked with the larger circles.

200 pc/kg of air.) In the high-altitude samples taken next, strong and weak ones alternated in an irregular way, but none comparable with sample L-212 was obtained. Sample L-212 could, from the γ-spectrometric measurements, be attributed to the tests of 30 September (*2*). The mixing with activity from earlier tests must have been insignificant, even for the weakest particles, and the sample was thus a very convenient one for study.

Examination of Debris from Explosion of 30 September

Thirty of the most strongly radioactive particles from sample L-212 and the accompanying sample from below the tropopause (L-211) were punched out, repeatedly measured with β- and, to some extent, γ-counters (*7*), and autoradiographed, with varying exposure times and at different ages.

The most strongly radioactive particles found, which caused the spots of millimeter diameter on the conventional autoradiographs, had a β-activity of a few nanocuries. Some of the curves for γ-decay are presented in Fig. 5, together with the curve for γ-decay for a sample of the whole filter.

In Fig. 6 the β-decay for a number of particles is plotted. It is obvious that this decay is of type $K \cdot t^{-k}$. The mean value for k for all the particles examined is 1.15, with a standard deviation of 0.15. This rate of decay corresponds well with the theoretical rate (*8*).

In addition to systematical variations with particle size (*9*) variations between individual particles of the same size were found.

In the plots of spot size versus activity no systematic variation with the age of the particles could be observed. Nor was there any indication that certain particles with an anomalous activity composition would fail to fit the plots. Some plots are shown in Fig. 3 together with the average plot, which is used as a standard curve for the activity measurements. When the standard curve is used, some strongly radioactive particles of a sample are both measured in a β-counter and autoradiographed. The standard plot is then displaced so as to give the best adaptation to the plotted points of these particles for each film. A small systematic error may arise for the less radioactive particles, as they do not have the same composition as the more radioactive ones (*9*). (According to the foregoing theory, the lower parts of the curve are not very sensitive to the energy of the β-particles.)

The relationship between particle size and activity was investigated, and microscopic examination was made of about a thousand particles from sample L-212. The great particle density on this filter made punching unnecessary; filter pieces of about 20 square centimeters each were leached with acetone, and the main part of the glass fibers was filtered away by a metal gauze of 200-micron mesh. Although the fiber residual retained 15 percent of the activity, it could be shown by autoradiograph that this activity contained less than 1 percent of the particles of sizes large enough to be seen under the microscope (>0.2 μ).

Results

The particles are colorless to reddish, translucent, and more or less spherical. Some characteristic particles are shown in Fig. 7. Activity versus size for about 1000 particles at an age of 120 days is shown in Fig. 8. About 30 percent of the particles were measured at an age of 45 days and projections of the measurements to 120 days were made by using the average disintegration slope for the 30 chosen particles mentioned above.

On account of variation in efficiency of the filter with particle size, the plot does not give a true picture of the particle size distribution, even if the 30 particles with strong β-activity and the lower part of the plot, where a great fraction of the particles in the sample are not represented, are excluded.

If we frame the "point-cloud" in Fig. 8 by two lines with the slope lying at a vertical distance representing a tenfold increase in activity, chosen by visual adapting, the cloud can be characterized by the symmetrical line between these two framing lines. Thus we have, for 120-day-old particles, $I = 6.7\ d^3$, when I is the β-activity in disintegrations per minute and d is the particle diameter in microns. Fourteen percent of the particles lie outside the framing lines—that is, the activities of these particles differ by more than a factor of $10^{1/2}$ from the activities derived with the formula given above.

By using the decay formula $I = K \cdot t^{-1.15}$, we have, for 100-day-old particles, $I = 8.4\ d^3$.

A more detailed description of this work has been given elsewhere (*10*).

References and Notes

1. K. Edvarson, "A Device for Air-Sampling in the Upper Atmosphere," *FOA 2 Rept. No. 2407–2097* (1957).
2. K. Löw, private communication.
3. H. Yagoda, *Radioactive Measurements with Nuclear Emulsions* (Wiley, New York, 1949).

J. Sisefsky, *Brit. J. Appl. Phys.* **10**, 526 (1959).

5. G. Hultqvist, *FOA 4 Rept. No. A 4174–4262* (1960).
6. M. Bååth, "Seismiska registreringar av explosioner, särskilt kärnvapenexplosioner, del II," *FOA 2 Rept. No. A 2020–2092* (1959).
7. The gamma-ray counter used was a 1¼- by 1-in. Na (T1) I crystal shielded by a 10-cm lead cover; background radiation, 36 count/min (above 30 kev) [efficiency, 0.15 Mev photons (Ce^{144}), 11 percent; 0.75 Mev (Zr^{95}), 5.8]. The β-counter used was constructed of β-end-window GM tube (7 mg of aluminum per square centimeter) shielded by γ counting GM tubes in anti-coincidence coupling and a 10-cm iron cover, which reduced the background radiation to 2 count/min. [An improved construction is described in (*5*).] The efficiency, which is hard to calculate because it varies with β-energy and thickness of the samples, has been estimated at 9 percent, on an average.
8. R. Bjornerstedt, *Arkiv Fysik* **16**, 293 (1959); ——— and K. Löw, *ibid.* **13**, 85 (1957).

K. Edvarson, K. Löw, J. Sisefsky, *Nature* **184**, 1771 (1959).

10. J. Sisefsky, "Autoradiographic and Microscopic Examination of Nuclear-Weapon Debris Particles," *FOA 4 Rept. No. A 4130–456* (1960).